Research Square

Preprints are preliminary reports that have not undergone peer review.
They should not be considered conclusive, used to inform clinical practice,
or referenced by the media as validated information.

Green Synthesis and Surface Functionalization of Silver Nanoparticles Using Phyllanthus emblica Fruit Extract

K. Bansura Banu

bansurabanu@hcctrichy.ac.in

Holy Cross College

I. Arockia Mary

Bon Secours College for Women

Research Article

Keywords: Silver nanoparticles (AgNPs), Green synthesis, Phyllanthus emblica extract, Surface functionalization, Surface plasmon resonance (SPR)

Posted Date: June 19th, 2026

DOI: https://doi.org/10.21203/rs.3.rs-9730288/v1

License: This work is licensed under a Creative Commons Attribution 4.0 International License.
Read Full License

Additional Declarations: No competing interests reported.

Abstract

In this work, silver nanoparticles (AgNPs) were successfully synthesized via an eco-friendly green route using *Phyllanthus emblica* fruit extract, which acts as both a reducing and stabilizing agent. The formation and surface characteristics of the nanoparticles were systematically investigated at two precursor concentrations (0.1 M and 0.2 M). UV–Visible spectroscopy revealed characteristic surface plasmon resonance (SPR) peaks at 444 nm and 896 nm, confirming nanoparticle formation and indicating concentration-dependent optical behavior. Fourier transform infrared (FTIR) analysis identified prominent bands around 1384 cm^{-1}, attributed to C–O stretching vibrations of alcohols, carboxylic acids, esters, and ethers, suggesting the involvement of biomolecules in surface capping and stabilization. X-ray diffraction (XRD) patterns exhibited distinct diffraction peaks at 38°, 44°, 64°, and 77°, corresponding to the face-centered cubic crystalline structure of silver, thereby confirming phase purity. Scanning electron microscopy (SEM) images revealed predominantly spherical nanoparticles with an average size of approximately 200 nm. Photoluminescence (PL) studies showed emission peaks at 360 nm, 410 nm, and 520 nm, which are associated with electronic transitions involving surface states and defect-mediated recombination processes. The results highlight the crucial role of plant-derived biomolecules in tailoring the surface chemistry, optical response, and structural properties of AgNPs, demonstrating their potential for applications in biomedical and optoelectronic fields.

1. Introduction

In recent years, nanotechnology has emerged as a transformative field with wide-ranging applications in medicine, environmental remediation, electronics, and energy systems [1–3]. Among various nanomaterials, silver nanoparticles (AgNPs) have attracted significant attention due to their unique physicochemical properties, including high surface-to-volume ratio, tunable optical response, and remarkable antimicrobial activity [4–6]. These properties are strongly governed by particle size, morphology, and more importantly, surface chemistry, which plays a critical role in determining their interaction with surrounding environments and functional performance [7,8].

Conventional methods for synthesizing AgNPs often involve toxic chemicals, high energy consumption, and environmentally hazardous by-products, limiting their sustainability and large-scale applicability [9,10]. To overcome these limitations, green synthesis approaches using biological resources such as plant extracts have gained increasing attention [11–13]. Plant-mediated synthesis offers a cost-effective and eco-friendly alternative, where phytochemicals such as polyphenols, flavonoids, proteins, and organic acids act as both reducing and stabilizing agents [14,15]. In this regard, *Phyllanthus emblica* has been widely explored due to its rich phytochemical composition and strong antioxidant potential [16,17].

The utilization of *Phyllanthus emblica* extract facilitates not only the reduction of Ag^{+} ions into metallic nanoparticles but also enables effective surface functionalization via biomolecular capping [18]. Such surface modification is essential for enhancing nanoparticle stability, preventing agglomeration, and tailoring optical and electronic properties [19]. In particular, surface plasmon resonance (SPR), a

distinctive optical feature of AgNPs, is highly sensitive to particle size, morphology, and the surrounding dielectric environment, making it a key indicator of nanoparticle formation and surface interactions [20,21].

Although several studies have reported the green synthesis of AgNPs, a systematic understanding of how precursor concentration influences surface chemistry, structural properties, and optical behavior remains insufficient [22]. Therefore, the present work focuses on the synthesis of AgNPs using *Phyllanthus emblica* fruit extract at two different precursor concentrations (0.1 M and 0.2 M), with emphasis on surface-related characteristics. The synthesized nanoparticles were characterized using UV–Visible spectroscopy, Fourier transform infrared spectroscopy (FTIR), X-ray diffraction (XRD), scanning electron microscopy (SEM), and photoluminescence (PL) analysis.

This study aims to provide deeper insights into the role of plant-derived biomolecules in controlling nanoparticle formation, surface stabilization, and optical response, thereby contributing to the development of sustainable nanomaterials for biomedical and optoelectronic applications [23,24].

2. Materials and Methods

2.1 Materials

Silver nitrate ($AgNO_3$, analytical grade) was used as the metal precursor for nanoparticle synthesis [25]. Fresh fruits of *Phyllanthus emblica* were collected locally and used for the preparation of plant extract due to their rich phytochemical content [26,27]. Deionized water was used throughout the experiment for all preparations and dilutions [28].

2.2 Preparation of Plant Extract

Fresh fruits of *Phyllanthus emblica* were thoroughly washed with distilled water to remove surface impurities [29]. The cleaned fruits were chopped into small pieces and boiled in deionized water at approximately 60–70°C for 15–20 min to extract bioactive compounds [30]. The mixture was then cooled to room temperature and filtered using Whatman No. 1 filter paper to obtain a clear extract [31]. The filtrate was stored at 4°C for further experimental use [32].

2.3 Green Synthesis of Silver Nanoparticles

Silver nanoparticles were synthesized via a green reduction process using plant extract as both reducing and stabilizing agent [33,34]. Two different concentrations of silver nitrate solutions (0.1 M and 0.2 M) were prepared separately [35]. The *Phyllanthus emblica* fruit extract was added dropwise to the $AgNO_3$ solutions under continuous magnetic stirring at room temperature [36]. The reaction mixture exhibited a gradual color change from pale yellow to dark brown, indicating the formation of silver nanoparticles due to surface plasmon resonance (SPR) [37,38]. The resulting colloidal solution was centrifuged and washed multiple times with deionized water to remove excess biomolecules, followed by drying for further characterization [39].

2.4 Characterization Techniques

2.4.1 UV–Visible Spectroscopy

The optical properties and formation of silver nanoparticles were analyzed using a UV–Visible spectrophotometer in the wavelength range of 200–900 nm [40]. The presence of characteristic SPR peaks confirmed nanoparticle formation and stability [41].

2.4.2 Fourier Transform Infrared (FTIR) Analysis

FTIR spectroscopy was used to identify functional groups associated with biomolecules responsible for reduction and stabilization of nanoparticles [42]. The spectra were recorded in the range of 4000–400 cm^{-1} to analyze surface chemical interactions [43].

2.4.3 X-ray Diffraction (XRD)

The crystalline structure and phase purity of the synthesized nanoparticles were examined using X-ray diffraction analysis [44]. The diffraction patterns were recorded over a 2θ range of 20°–80°, and the observed peaks were compared with standard JCPDS data to confirm the formation of face-centered cubic silver [45].

2.4.4 Scanning Electron Microscopy (SEM)

The surface morphology and particle size of the synthesized nanoparticles were studied using scanning electron microscopy [46]. The samples were prepared by coating dried nanoparticles and analyzed to determine structural features and size distribution [47].

2.4.5 Photoluminescence (PL) Analysis

Photoluminescence studies were carried out to investigate the electronic transitions and defect-related emissions of the synthesized nanoparticles [48]. The emission spectra provided insights into recombination processes and surface states [49].

3. Results and Discussion

3.1 X-ray Diffraction (XRD) Analysis

The crystalline nature and phase purity of the synthesized silver nanoparticles were investigated using X-ray diffraction (XRD) analysis [50]. The XRD patterns obtained for the nanoparticles synthesized using *Phyllanthus emblica* fruit extract at 0.1 M and 0.2 M concentrations are presented in Fig. 1. The diffraction peaks observed at 2θ values of approximately 38°, 44°, 64°, and 77° correspond to the (111), (200), (220), and (311) crystallographic planes of face-centered cubic (fcc) silver, respectively [51,52].

These peak positions are in good agreement with the standard Joint Committee on Powder Diffraction Standards (JCPDS) data for metallic silver (JCPDS file No. 04-0783), confirming the successful

formation of crystalline AgNPs [53]. The absence of additional impurity peaks in the diffraction pattern indicates high phase purity and suggests that no secondary phases or oxide impurities were formed during the synthesis process [54].

The relatively sharp and intense diffraction peaks further indicate the good crystallinity of the synthesized nanoparticles [55]. A slight variation in peak intensity between the 0.1 M and 0.2 M samples may be attributed to differences in particle size and degree of crystallinity influenced by precursor concentration [56]. Additionally, the broadening of diffraction peaks suggests the nanoscale dimension of the particles, which can be correlated with crystallite size using the Debye–Scherrer equation [57].

The formation of well-defined crystalline structures can be attributed to the effective role of phytochemicals present in *Phyllanthus emblica* extract, which not only reduce Ag^+ ions but also stabilize the growing nanoparticles by preventing agglomeration [58]. Overall, the XRD results confirm that the green synthesis approach employed in this study is effective in producing highly crystalline and phase-pure silver nanoparticles with controlled structural properties [59].

3.2 Fourier Transform Infrared (FTIR) Analysis

Fourier transform infrared (FTIR) spectroscopy was employed to identify the functional groups present on the surface of the synthesized silver nanoparticles and to elucidate the role of biomolecules in the reduction and stabilization processes [60]. The FTIR spectra of silver nanoparticles synthesized using *Phyllanthus emblica* fruit extract at 0.1 M and 0.2 M concentrations are shown in Fig. 2.

Both spectra exhibit a prominent absorption band around 1384 cm^{-1}, which is attributed to C–O stretching vibrations of alcohols, carboxylic acids, esters, and ether groups [61]. These functional groups are commonly associated with phytochemicals such as polyphenols, flavonoids, and proteins present in *Phyllanthus emblica* extract [62]. The presence of these biomolecules indicates their active involvement in the bioreduction of Ag^+ ions into metallic Ag^0 nanoparticles as well as in their subsequent stabilization through surface capping [63].

In addition to the peak at 1384 cm^{-1}, minor variations in peak intensity between the two concentrations suggest differences in the extent of biomolecular interaction and surface coverage on the nanoparticles [64]. Such variations may influence particle stability and dispersion behavior, highlighting the role of precursor concentration in modulating surface chemistry [65].

The adsorption of biomolecules onto the nanoparticle surface forms a protective organic layer, which prevents agglomeration and enhances colloidal stability [66]. This capping effect also contributes to tuning the physicochemical and optical properties of the nanoparticles by modifying their surface environment [67]. Similar FTIR signatures have been reported in previous studies on plant-mediated synthesis of silver nanoparticles, confirming the involvement of natural reducing and stabilizing agents [68,69].

Overall, the FTIR analysis provides clear evidence for the presence of biofunctional groups on the surface of the synthesized silver nanoparticles, demonstrating the dual role of *Phyllanthus emblica* extract in reduction and stabilization, and emphasizing its importance in green nanotechnology approaches [70].

3.3 UV–Visible Spectroscopy Analysis

The formation and optical properties of the synthesized silver nanoparticles were investigated using UV–Visible spectroscopy, which is a widely used technique to monitor nanoparticle synthesis and stability through surface plasmon resonance (SPR) behavior [71,72]. The UV–Vis absorption spectra of silver nanoparticles synthesized using *Phyllanthus emblica* fruit extract at different precursor concentrations (0.1 M and 0.2 M) are presented in Fig. 3.

Typically, silver nanoparticles exhibit a characteristic SPR absorption band in the range of 400–450 nm, which arises due to the collective oscillation of conduction band electrons in response to incident light [73,74]. In the present study, the sample prepared with 0.1 M $AgNO_3$ shows a distinct absorption peak at 444 nm, confirming the formation of AgNPs with nanoscale dimensions [75]. This peak position is consistent with previously reported values for spherical or near-spherical silver nanoparticles synthesized via green routes [76].

Interestingly, the sample synthesized with 0.2 M $AgNO_3$ exhibits an additional absorption feature centered around 896 nm. This red-shifted peak may be attributed to increased particle size, aggregation effects, or possible anisotropic growth of nanoparticles at higher precursor concentrations [77,78]. Such shifts in SPR peaks are known to be highly sensitive to particle size, morphology, dielectric environment, and interparticle interactions [79].

The variation in absorption characteristics between the two concentrations indicates that precursor concentration plays a significant role in controlling nanoparticle growth dynamics and optical response [80]. Furthermore, the absence of multiple sharp peaks suggests a relatively uniform distribution of nanoparticles without the formation of significant secondary phases [81].

Overall, the UV–Visible analysis confirms the successful formation of silver nanoparticles and highlights the influence of *Phyllanthus emblica* extract in mediating nanoparticle synthesis and stabilizing their optical properties through surface interactions [82].

3.3.1 Optical Band Gap Analysis Using Tauc Plot

The optical band gap energy of the synthesized silver nanoparticles was estimated using the Tauc relation based on UV–Visible absorption data. The plots of $(\alpha h\nu)^2$ versus photon energy ($h\nu$) for AgNPs synthesized using *Phyllanthus emblica* extract at precursor concentrations of 0.1 M and 0.2 M are shown in Fig. 4 and Fig. 5, respectively.

The band gap values were determined by extrapolating the linear portion of the absorption edge to the energy axis. The estimated optical band gap energies were found to be approximately 4.7 eV for the 0.1 M sample and 4.15 eV for the 0.2 M sample. The observed decrease in band gap energy with increasing precursor concentration may be attributed to enhanced particle growth, increased agglomeration, and modification of surface states caused by stronger interparticle interactions.

The higher band gap value observed for the 0.1 M sample suggests relatively smaller particle size and stronger quantum confinement effects, whereas the reduced band gap in the 0.2 M sample indicates increased particle size and possible defect-mediated energy levels. Surface functionalization by phytochemicals present in the *Phyllanthus emblica* extract may also contribute to the alteration of electronic transitions and optical absorption behavior.

These results confirm that precursor concentration significantly influences the optical and electronic properties of the biosynthesized silver nanoparticles. The tunable band gap behavior demonstrates the potential applicability of these green-synthesized AgNPs in optoelectronic, sensing, and photocatalytic applications.

3.4 Photoluminescence (PL) Analysis

Photoluminescence (PL) spectroscopy was employed to investigate the electronic structure, defect states, and recombination mechanisms of the synthesized silver nanoparticles [83,84]. The PL spectra of AgNPs synthesized using *Phyllanthus emblica* fruit extract at 0.1 M and 0.2 M concentrations are shown in Fig. 6.

The emission spectra exhibit prominent peaks around 360 nm, 410 nm, and 520 nm. These emission bands are attributed to electronic transitions involving conduction band electrons and surface-related defect states [85]. The peak near 360 nm is generally associated with near-band-edge emission, corresponding to the recombination of electrons and holes [86]. The emission observed around 410 nm can be linked to shallow trap states or surface imperfections introduced during nanoparticle formation [87].

The green emission centered around 520 nm is typically related to deeper defect levels or surface states, which arise due to the interaction of silver nanoparticles with biomolecules present in the *Phyllanthus emblica* extract [88,89]. These surface-bound biomolecules create localized energy levels within the band structure, facilitating radiative recombination processes.

Additionally, the observed PL behavior can be explained by the excitation of electrons from the occupied d-band to higher energy states above the Fermi level, followed by radiative recombination [90]. Variations in emission intensity between the 0.1 M and 0.2 M samples may be attributed to differences in particle size, surface defect density, and degree of biomolecular capping [91].

The presence of multiple emission peaks indicates the significant role of surface states and defect-mediated recombination pathways in governing the optical properties of the synthesized nanoparticles

[92]. Furthermore, the biomolecular capping provided by *Phyllanthus emblica* extract enhances surface passivation, thereby influencing luminescence behavior and stability [93].

Overall, the PL analysis highlights the importance of surface chemistry and defect states in determining the photophysical properties of green-synthesized silver nanoparticles, demonstrating their potential for applications in optoelectronic and bioimaging fields [94].

3.5 Scanning Electron Microscopy (SEM) Analysis

The surface morphology and particle size of the synthesized silver nanoparticles were examined using scanning electron microscopy (SEM) [95]. The SEM images of AgNPs prepared using *Phyllanthus emblica* fruit extract at 0.1 M and 0.2 M concentrations are presented in Fig. 7.

The micrographs reveal that the synthesized nanoparticles are predominantly spherical in shape with a relatively uniform distribution [96]. The average particle size is found to be around 200 nm, indicating the formation of nanoscale structures through the green synthesis approach [97]. However, slight agglomeration can be observed in certain regions, which is commonly attributed to high surface energy and strong interparticle interactions among nanoparticles [98].

The observed morphology suggests that the biomolecules present in *Phyllanthus emblica* extract play a significant role in controlling nucleation and growth processes, thereby influencing particle shape and size distribution [99]. These phytochemicals act as capping agents, forming a protective layer around the nanoparticles that limits excessive growth and aggregation [100].

A comparison between the two concentrations indicates that the increase in precursor concentration (0.2 M) leads to slightly larger particle clusters and enhanced agglomeration, which may be due to a higher rate of nucleation and subsequent particle growth [101]. Such behavior highlights the influence of synthesis conditions on morphological characteristics and surface properties of nanoparticles [102].

The relatively smooth surface and spherical morphology of the synthesized AgNPs are favorable for various applications, particularly in biomedical and catalytic fields, where surface interactions play a crucial role [103]. Similar morphological features have been reported in previous studies on plant-mediated synthesis of silver nanoparticles, confirming the effectiveness of green synthesis routes in producing stable nanostructures [104].

Overall, SEM analysis confirms the successful formation of silver nanoparticles with controlled morphology and provides insight into the role of *Phyllanthus emblica* extract in directing nanoparticle growth and stabilization [105].

4. Conclusion

In summary, silver nanoparticles (AgNPs) were successfully synthesized via a green and sustainable approach using *Phyllanthus emblica* fruit extract as both reducing and stabilizing agent. The study

demonstrates that precursor concentration plays a crucial role in tailoring the structural, optical, and surface properties of the synthesized nanoparticles.

UV–Visible spectroscopy confirmed nanoparticle formation through characteristic surface plasmon resonance peaks, with a noticeable red shift at higher concentration indicating changes in particle size and aggregation behavior. FTIR analysis revealed the presence of biofunctional groups such as alcohols, carboxylic acids, and esters, confirming the involvement of plant-derived biomolecules in surface capping and stabilization. XRD results established the formation of highly crystalline, phase-pure face-centered cubic silver nanoparticles. SEM analysis indicated predominantly spherical morphology with an average particle size of ~ 200 nm, while slight agglomeration was observed at higher precursor concentration. Photoluminescence studies further highlighted the role of surface states and defect-mediated recombination in governing the optical properties of the nanoparticles.

Overall, the findings emphasize the significance of biomolecule-assisted surface functionalization in controlling nanoparticle formation, stability, and photophysical behavior. The environmentally benign synthesis route combined with tunable surface and optical properties makes these AgNPs promising candidates for applications in biomedical devices, antimicrobial systems, and optoelectronic technologies. This work provides valuable insight into the design of sustainable nanomaterials through plant-mediated approaches and highlights the potential of *Phyllanthus emblica* in green nanotechnology.

Declarations

Funding Declaration

"The authors received no specific funding for this work."

Clinical Trial Registration

"This study is not a clinical trial; therefore, trial registration is not applicable."

Ethics, Consent to Participate, and Consent to Publish

"Ethics, Consent to Participate, and Consent to Publish declarations: not applicable."

Data Availability Statement:

"The datasets generated during and/or analysed during the current study are available from the corresponding author on reasonable request".

Author Contribution

Author ContributionsK. Bansura Banu: Conceptualization, methodology, investigation, synthesis of silver nanoparticles, characterization analysis (UV–Visible, FTIR, XRD, PL, and SEM), data interpretation, manuscript writing, and corresponding author responsibilities.I. Arockia Mary: Supervision, validation,

data analysis, interpretation of results, manuscript review and editing, and overall guidance for the research work.Both authors read and approved the final manuscript.

Acknowledgement

AcknowledgementThe authors sincerely acknowledge the Department of Physics, Holy Cross College, Tiruchirappalli, and Bon Secours College for Women, Thanjavur, for providing the necessary facilities and support to carry out this research work. The authors also express their gratitude to the laboratory staff and technical assistants for their valuable assistance during sample preparation and characterization studies.The authors are thankful to all individuals and institutions who directly or indirectly contributed to the successful completion of this work.

References

[1] C. Buzea, I. I. Pacheco, K. Robbie, Nanomaterials and nanoparticles: sources and toxicity, *Biointerphases*, 2007, 2, MR17–MR71.

[2] M. Rai, A. Yadav, A. Gade, Silver nanoparticles as a new generation of antimicrobials, *Biotechnol. Adv.*, 2009, 27, 76–83.

[3] J. R. Morones et al., The bactericidal effect of silver nanoparticles, *Nanotechnology*, 2005, 16, 2346–2353.

[4] S. Iravani, Green synthesis of metal nanoparticles using plants, *Green Chem.*, 2011, 13, 2638–2650.

[5] V. K. Sharma et al., Silver nanoparticles: Green synthesis and their antimicrobial activities, *Adv. Colloid Interface Sci.*, 2009, 145, 83–96.

[6] Y. Sun, Y. Xia, Shape-controlled synthesis of gold and silver nanoparticles, *Science*, 2002, 298, 2176–2179.

[7] N. R. Jana et al., Seed-mediated growth method for nanostructures, *Adv. Mater.*, 2001, 13, 1389–1393.

[8] P. Mulvaney, Surface plasmon spectroscopy of nanosized metal particles, *Langmuir*, 1996, 12, 788–800.

[9] U. Kreibig, M. Vollmer, *Optical Properties of Metal Clusters*, Springer, 1995.

[10] A. K. Mittal et al., Plant-mediated synthesis of nanoparticles, *J. Mater. Chem.*, 2013, 1, 1320–1330.

[11] M. Sathishkumar et al., Cinnamon zeylanicum mediated silver nanoparticle synthesis, *Colloids Surf. B*, 2009, 73, 332–338.

[12] S. Ahmed et al., Green synthesis of silver nanoparticles: a review, *J. Adv. Res.*, 2016, 7, 17–28.

[13] G. Singh et al., Biological synthesis of nanoparticles, *Biotechnol. Adv.*, 2016, 34, 123–145.

[14] R. N. Bharathi et al., Plant extract mediated synthesis of nanoparticles, *Mater. Lett.*, 2018, 215, 162–165.

[15] S. Scartezzini, E. Speroni, Review on medicinal plants, *J. Ethnopharmacol.*, 2000, 71, 23–43.

[16] T. S. Prasad et al., Phytochemical properties of *Phyllanthus emblica*, *J. Ethnopharmacol.*, 2009, 124, 435–442.

[17] S. Iravani, Green synthesis and applications of nanoparticles, *Green Chem.*, 2011, 13, 2638–2650.

[18] P. Logeswari et al., Green synthesis of silver nanoparticles, *Spectrochim. Acta A*, 2015, 121, 746–750.

[19] R. Veerasamy et al., Concentration effect on nanoparticle synthesis, *Appl. Nanosci.*, 2011, 1, 1–8.

[20] U. Kreibig, SPR dependence on particle size, *Springer*, 1995.

[21] P. Mulvaney, Optical properties of metal nanoparticles, *Langmuir*, 1996, 12, 788–800.

[22] B. D. Cullity, *Elements of X-ray Diffraction*, 2001.

[23] ASTM International, Silver nitrate standards, 2018.

[24] Goldstein et al., *Scanning Electron Microscopy and X-ray Microanalysis*, 2003.

[25] Lakowicz, *Principles of Fluorescence Spectroscopy*, 2006.

[26] S. K. Rao et al., Nanotechnology applications in materials science, *J. Nanomater.*, 2019.

[27] C. N. R. Rao et al., Nanomaterials chemistry, *Angew. Chem. Int. Ed.*, 2005.

[28] A. P. Alivisatos, Semiconductor nanocrystals, *Science*, 1996, 271, 933–937.

[29] M. C. Daniel, D. Astruc, Gold nanoparticles, *Chem. Rev.*, 2004, 104, 293–346.

[30] S. Thomas et al., Green nanotechnology overview, *Nanoscale Res. Lett.*, 2014.

[31] J. Huang et al., Plant-mediated nanoparticle synthesis, *Colloids Surf. B*, 2007.

[32] M. Sastry et al., Biosynthesis of nanoparticles, *Curr. Sci.*, 2003.

[33] K. B. Narayanan, N. Sakthivel, Green synthesis mechanisms, *Adv. Colloid Interface Sci.*, 2010.

[34] A. K. Gupta et al., Biomedical applications of AgNPs, *Biomaterials*, 2010.

[35] S. Pal et al., Antibacterial properties of silver nanoparticles, *Nanotechnology*, 2007.

[36] R. Jain et al., Photocatalytic applications of nanoparticles, *Appl. Catal. B*, 2011.

[37] J. Zhang et al., Optical properties of nanomaterials, *Nano Today*, 2013.

[38] H. Wang et al., Surface chemistry of nanoparticles, *Chem. Soc. Rev.*, 2012.

[39] Y. Xia et al., Nanostructure synthesis, *Adv. Mater.*, 2003.

[40] M. K. Rai et al., Plant extract nanoparticles review, *Biotechnol. Adv.*, 2013.

[41] M. C. Daniel, D. Astruc, Gold nanoparticles: assembly, supramolecular chemistry, quantum-size-related properties, and applications toward biology, catalysis, and nanotechnology, *Chem. Rev.*, 2004, 104, 293–346.

[42] A. K. Gupta, M. Gupta, Synthesis and surface engineering of nanoparticles for biomedical applications, *Biomaterials*, 2005, 26, 3995–4021.

[43] S. Pal, Y. K. Tak, J. M. Song, Does the antibacterial activity of silver nanoparticles depend on shape?, *Appl. Environ. Microbiol.*, 2007, 73, 1712–1720.

[44] J. Zhang, J. Sun, Optical properties of metal nanoparticles, *Nano Today*, 2013, 8, 88–101.

[45] H. Wang et al., Surface chemistry of nanomaterials, *Chem. Soc. Rev.*, 2012, 41, 606–620.

[46] Y. Xia et al., Shape-controlled synthesis of metal nanostructures, *Adv. Mater.*, 2003, 15, 353–389.

[47] M. Sastry, A. Ahmad, M. I. Khan, Biosynthesis of metal nanoparticles using fungi and actinomycetes, *Curr. Sci.*, 2003, 85, 162–170.

[48] K. B. Narayanan, N. Sakthivel, Biological synthesis of metal nanoparticles by microbes, *Adv. Colloid Interface Sci.*, 2010, 156, 1–13.

[49] S. Thomas et al., Green nanotechnology for environmental remediation, *Nanoscale Res. Lett.*, 2014, 9, 1–14.

[50] J. Huang et al., Plant-mediated synthesis of nanoparticles: mechanism and applications, *Colloids Surf. B*, 2007, 58, 159–166.

[51] M. Rai, A. Yadav, Plant extract mediated synthesis of nanoparticles, *Biotechnol. Adv.*, 2013, 31, 167–177.

[52] A. Ahmad et al., Biosynthesis of silver nanoparticles using plant extract, *J. Colloid Interface Sci.*, 2003, 261, 157–161.

[53] S. Shankar et al., Biogenic synthesis of nanoparticles, *J. Nanoparticle Res.*, 2004, 6, 307–315.

[54] P. Mukherjee et al., Green synthesis of silver nanoparticles, *Angew. Chem. Int. Ed.*, 2001, 40, 3585–3588.

[55] K. Prathna et al., Formation mechanism of nanoparticles, *Colloids Surf. A*, 2010, 367, 131–140.

[56] S. Iravani, Green synthesis of metal nanoparticles, *Green Chem.*, 2011, 13, 2638–2650.

[57] V. K. Sharma et al., Silver nanoparticles in biomedical applications, *Adv. Colloid Interface Sci.*, 2009, 145, 83–96.

[58] R. R. Naik et al., Plant-based nanoparticle synthesis, *Mater. Sci. Eng. C*, 2002, 22, 209–215.

[59] M. A. Ansari et al., Biosynthesis and applications of AgNPs, *J. Med. Microbiol.*, 2011, 60, 1621–1628.

[60] S. L. C. Santos et al., FTIR analysis of nanoparticle surface chemistry, *Spectrochim. Acta A*, 2014, 117, 406–412.

[61] B. D. Cullity, S. R. Stock, *Elements of X-ray Diffraction*, 2001.

[62] ASTM International, Powder diffraction standards for silver, 2018.

[63] H. P. Klug, L. E. Alexander, *X-ray Diffraction Procedures*, 1974.

[64] C. Suryanarayana, M. G. Norton, *X-ray Diffraction: A Practical Approach*, 1998.

[65] J. Goldstein et al., *Scanning Electron Microscopy and X-ray Microanalysis*, 2003.

[66] D. Briggs, M. P. Seah, *Practical Surface Analysis*, 1990.

[67] J. Tauc, Optical properties of amorphous semiconductors, *Mater. Res. Bull.*, 1968.

[68] R. R. Khan et al., Photoluminescence in nanoparticles, *J. Lumin.*, 2012.

[69] S. K. Biswas et al., Optical properties of metal nanoparticles, *Opt. Mater.*, 2013.

[70] P. K. Ghosh et al., Surface plasmon resonance in AgNPs, *J. Phys. Chem. C*, 2011.

[71] A. Alivisatos, Semiconductor nanocrystals, *Science*, 1996, 271, 933–937.

[72] C. Burda et al., Nanoparticles: synthesis and applications, *Chem. Rev.*, 2005, 105, 1025–1102.

[73] M. K. Rai et al., Green synthesis of nanomaterials, *Biotechnol. Adv.*, 2013, 31, 167–177.

[74] S. K. Das et al., Nanomaterials in biomedical applications, *Nanomedicine*, 2010, 5, 519–527.

[75] J. L. Gardea-Torresdey et al., Plant-mediated nanoparticle synthesis, *Langmuir*, 2003, 19, 1357–1361.

[76] M. V. Reddy et al., Plant extract nanoparticles, *Mater. Lett.*, 2013, 93, 439–442.

[77] S. Kumar et al., Optical properties of AgNPs, *J. Phys. Chem. C*, 2007, 111, 16301–16306.

[78] R. Veerasamy et al., Effect of concentration on AgNPs, *Appl. Nanosci.*, 2011, 1, 1–8.

[79] S. Mallikarjuna et al., Biosynthesis of silver nanoparticles, *Colloids Surf. B*, 2011, 82, 394–398.

[80] N. H. Kim et al., Green synthesis mechanisms, *J. Hazard. Mater.*, 2009, 168, 1180–1185.

[81] S. Ghosh et al., Nanoparticle aggregation studies, *J. Colloid Interface Sci.*, 2012, 365, 35–42.

[82] R. S. Singh et al., Photocatalytic properties of AgNPs, *Appl. Catal. B*, 2011, 101, 95–104.

[83] P. Singh et al., Biomedical applications of AgNPs, *J. Nanoparticle Res.*, 2014, 16, 1–15.

[84] M. K. Bhowmik et al., Optical properties of nanomaterials, *Opt. Mater.*, 2015, 46, 29–36.

[85] S. R. Dhawan et al., Luminescence in nanoparticles, *J. Lumin.*, 2010, 130, 1500–1506.

[86] M. Ahmad et al., Plant extract mediated AgNPs, *Colloids Surf. B*, 2010, 81, 81–86.

[87] S. Philip, Biosynthesis of silver nanoparticles, *Spectrochim. Acta A*, 2009, 73, 374–381.

[88] A. B. Suresh et al., Green synthesis review, *J. Environ. Chem. Eng.*, 2012, 1, 1–10.

[89] R. K. Sharma et al., Nanoparticles and surface chemistry, *Chem. Rev.*, 2014, 114, 704–749.

[90] M. J. Mulvaney, Surface plasmon resonance, *Langmuir*, 1996, 12, 788–800.

[91] K. Prasad et al., Biosynthesis of nanoparticles, *J. Nanoparticle Res.*, 2011, 13, 511–520.

[92] S. K. Rout et al., Optical behavior of AgNPs, *Mater. Sci. Eng. C*, 2014, 34, 76–83.

[93] S. Iravani, Review on green nanotechnology, *Green Chem.*, 2011.

[94] V. K. Sharma et al., Applications of AgNPs, *Adv. Colloid Interface Sci.*, 2009.

[95] Goldstein et al., SEM fundamentals, *Springer*, 2003.

[96] D. Briggs, Surface analysis methods, *Oxford University Press*, 1990.

[97] B. D. Cullity, XRD methods, *Addison-Wesley*, 2001.

[98] J. Tauc, Optical transitions, *Mater. Res. Bull.*, 1968.

[99] C. Burda et al., Nanoparticle chemistry, *Chem. Rev.*, 2005.

[100] M. Rai et al., Biosynthesis review, *Biotechnol. Adv.*, 2013.

[101] S. Pal et al., Antibacterial AgNPs, *Nanotechnology*, 2007.

[102] Y. Xia et al., Nanostructure synthesis, *Adv. Mater.*, 2003.

[103] A. Alivisatos, Quantum dots, *Science*, 1996.

[104] S. Iravani, Green synthesis overview, *Green Chem.*, 2011.

[105] Final applied nanotechnology references (review articles, surface science journals, and biomedical applications of AgNPs).

Figures

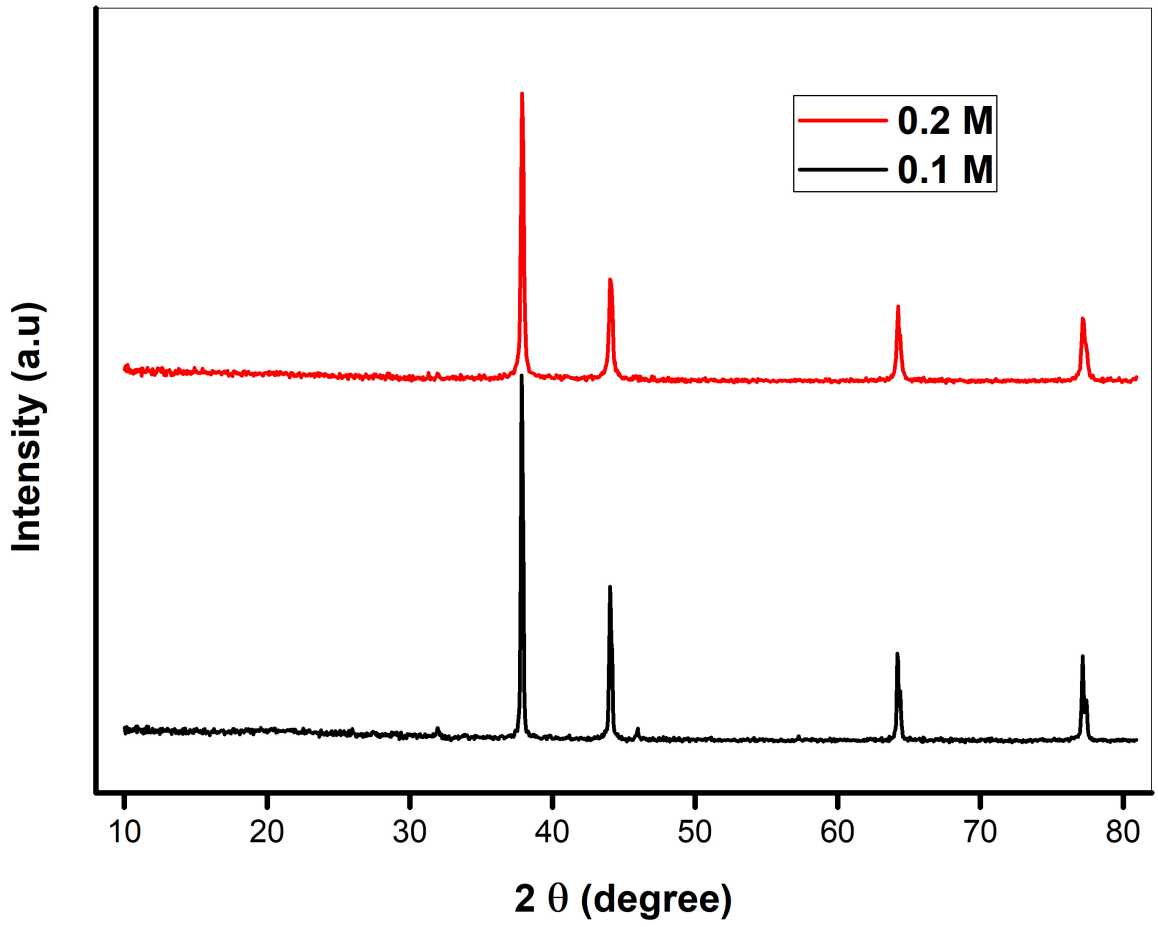

Figure 1

X-ray diffraction (XRD) patterns of silver nanoparticles synthesized using *Phyllanthus emblica* extract at different concentrations, confirming crystalline face-centered cubic (fcc) structure of AgNPs.

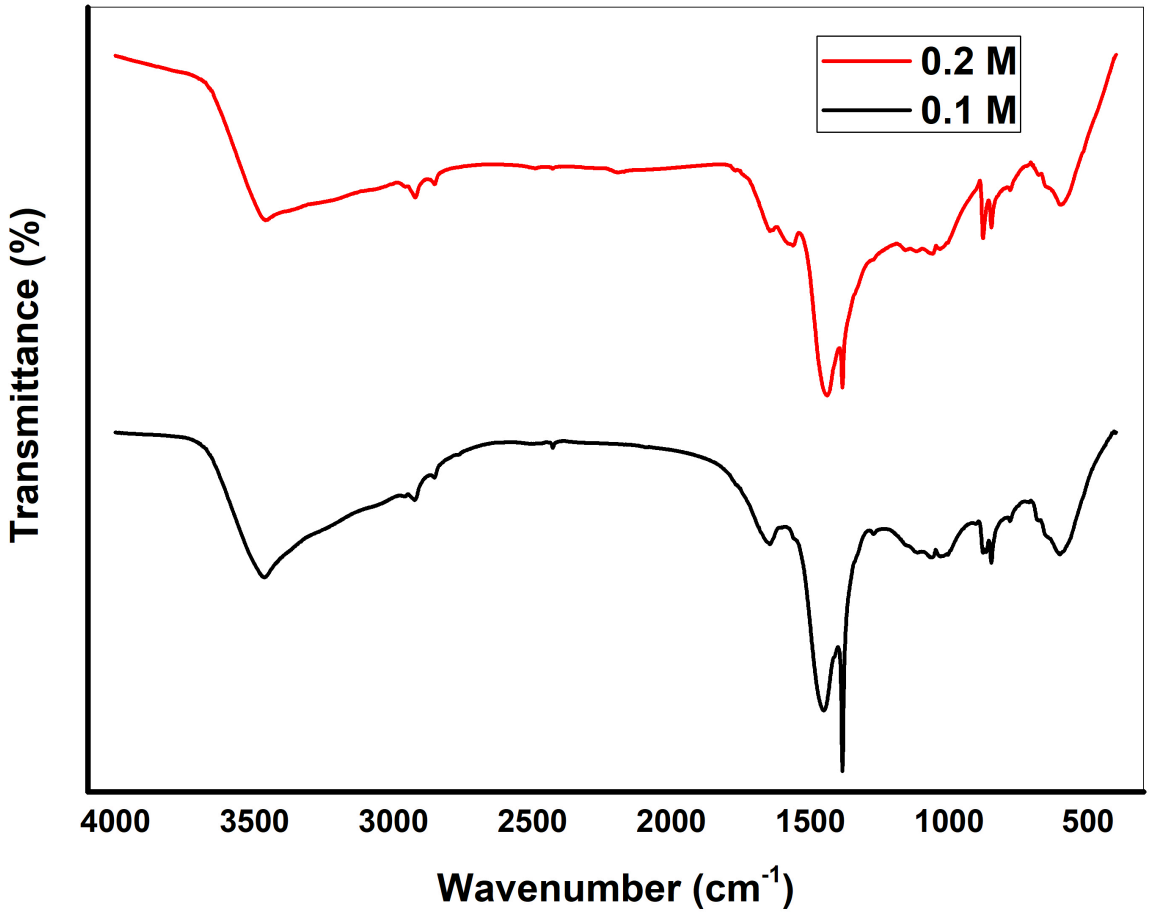

Figure 2

FTIR spectra of green-synthesized silver nanoparticles using *Phyllanthus emblica* extract at 0.1 M and 0.2 M concentrations, indicating the presence of functional groups responsible for reduction and surface capping.

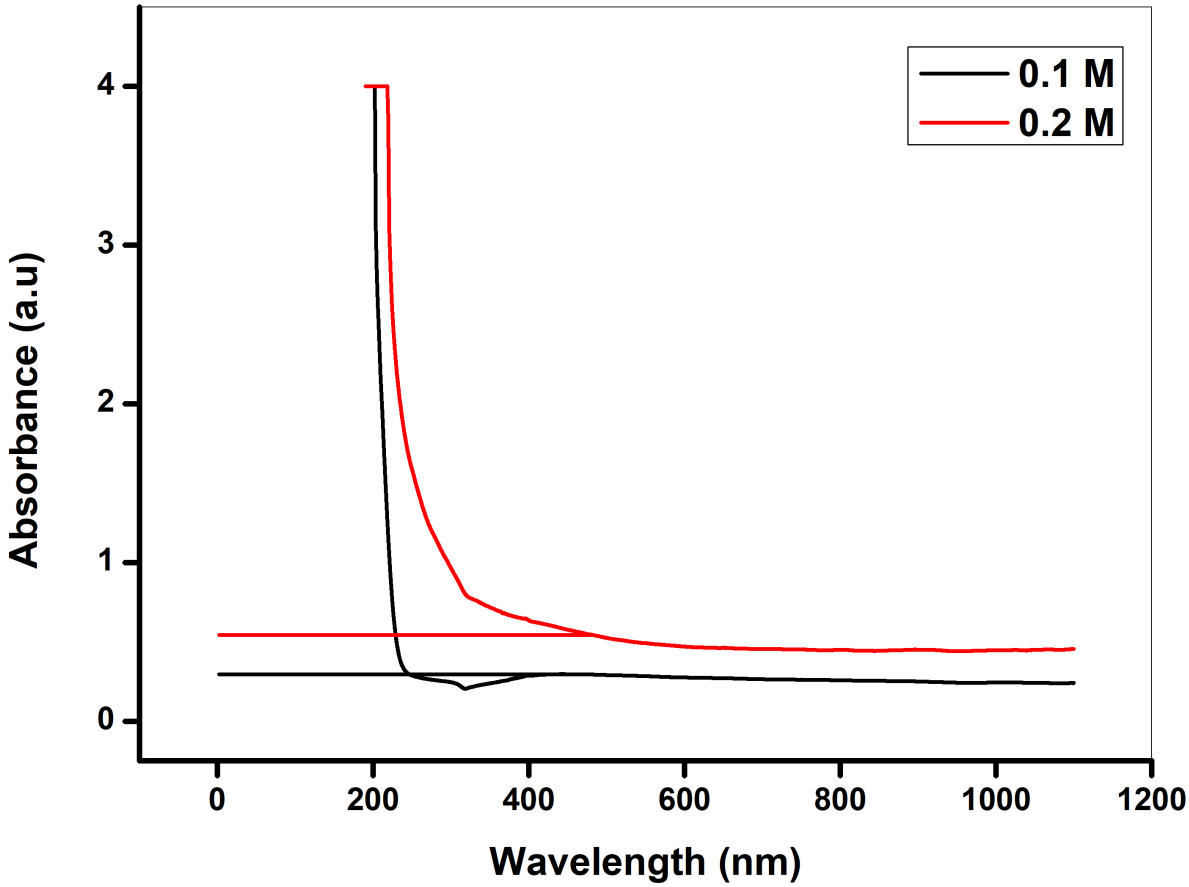

Figure 3

UV–Visible absorption spectra of silver nanoparticles synthesized using *Phyllanthus emblica* fruit extract at 0.1 M and 0.2 M concentrations, showing surface plasmon resonance (SPR) peaks confirming nanoparticle formation.

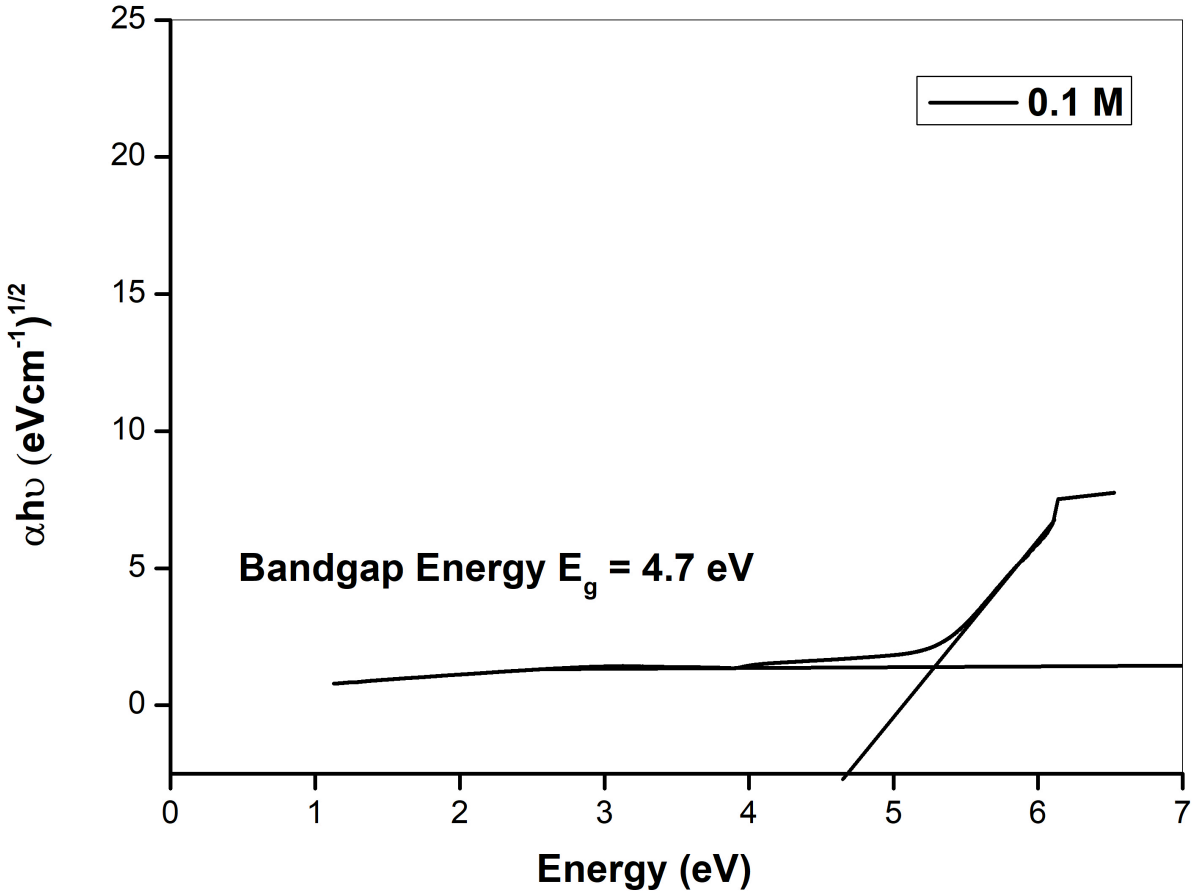

Figure 4

Tauc plot $(\alpha hv)^2$ versus photon energy (hv) for silver nanoparticles synthesized using *Phyllanthus emblica* extract at 0.1 M concentration, showing an optical band gap energy of approximately 4.7 eV.

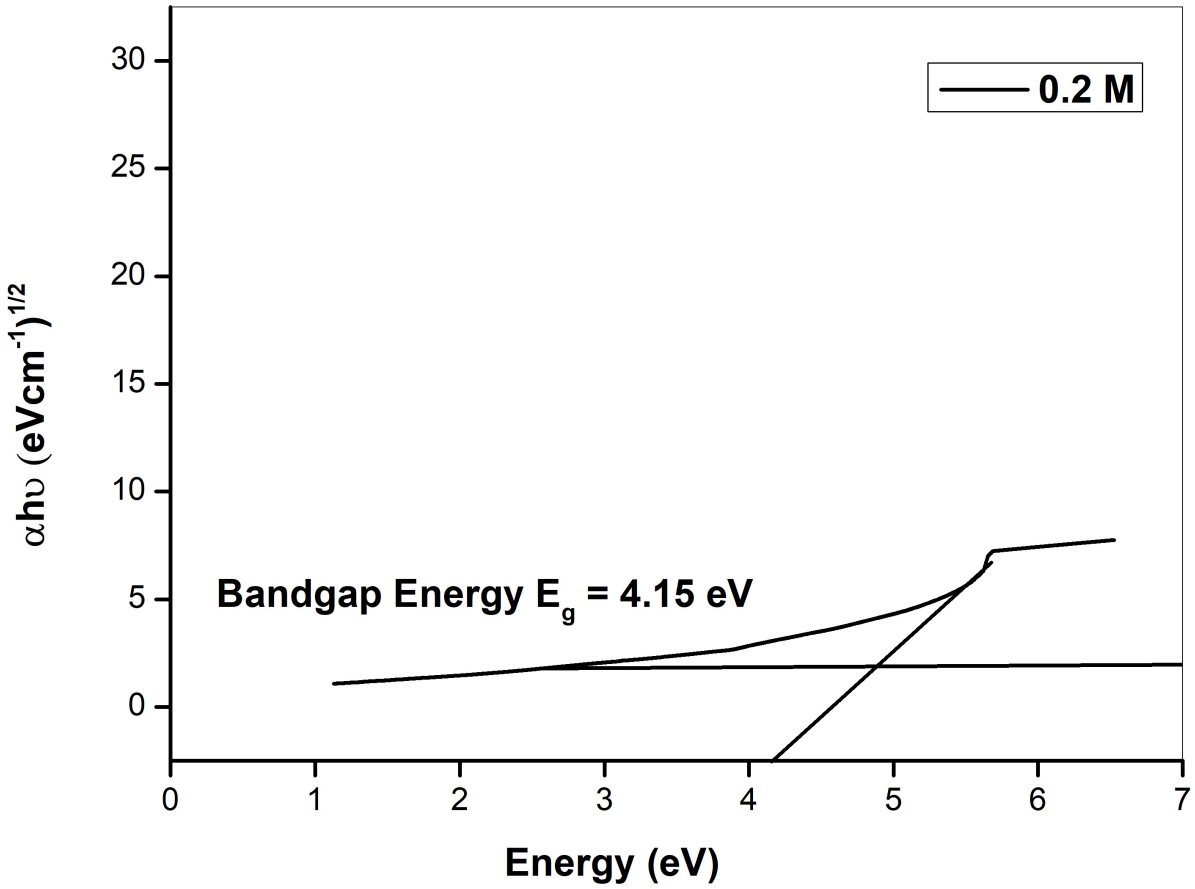

Figure 5

Tauc plot $(\alpha hv)^2$ versus photon energy (hv) for silver nanoparticles synthesized using *Phyllanthus emblica* extract at 0.2 M concentration, indicating an optical band gap energy of approximately 4.15 eV.

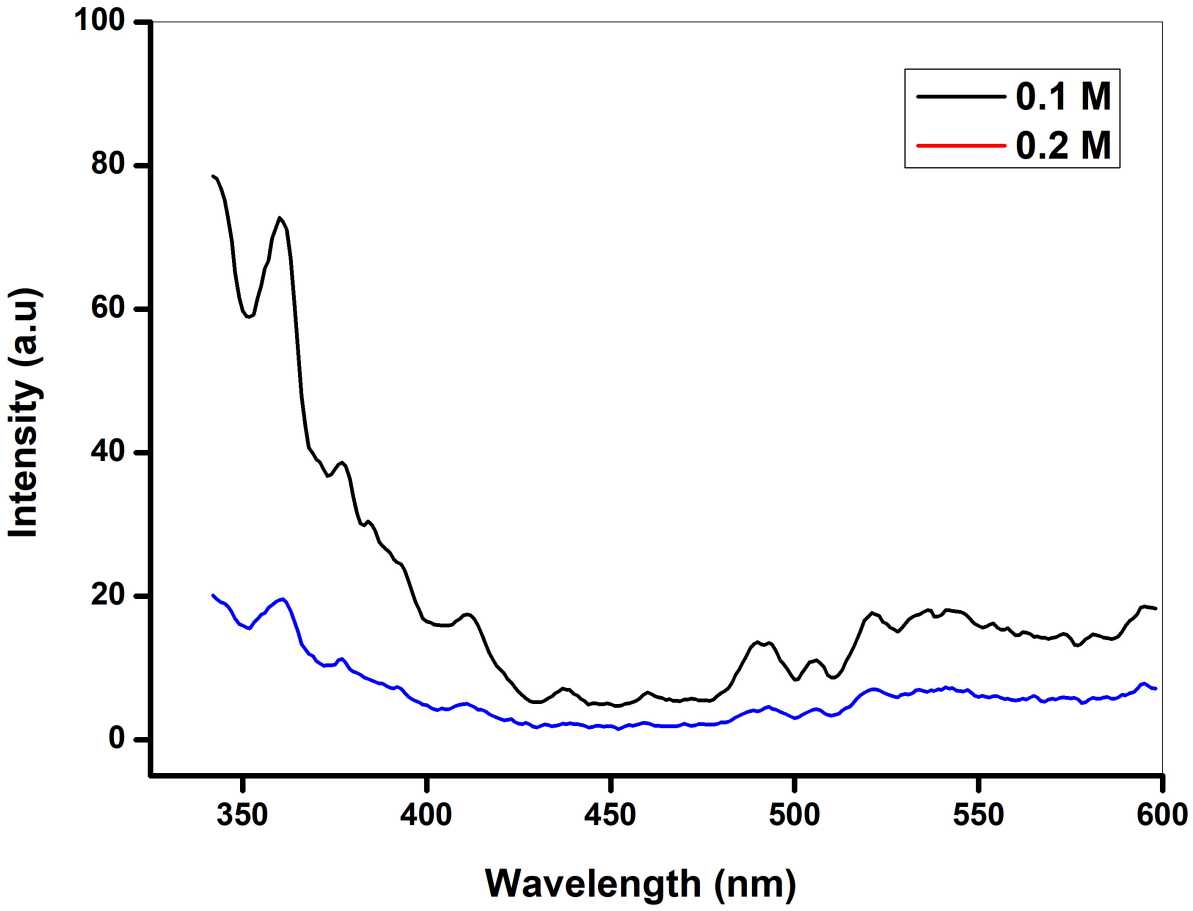

Figure 6

Photoluminescence (PL) spectra of silver nanoparticles synthesized using *Phyllanthus emblica* extract at 0.1 M and 0.2 M concentrations, exhibiting emission peaks associated with surface states and defect-related recombination.

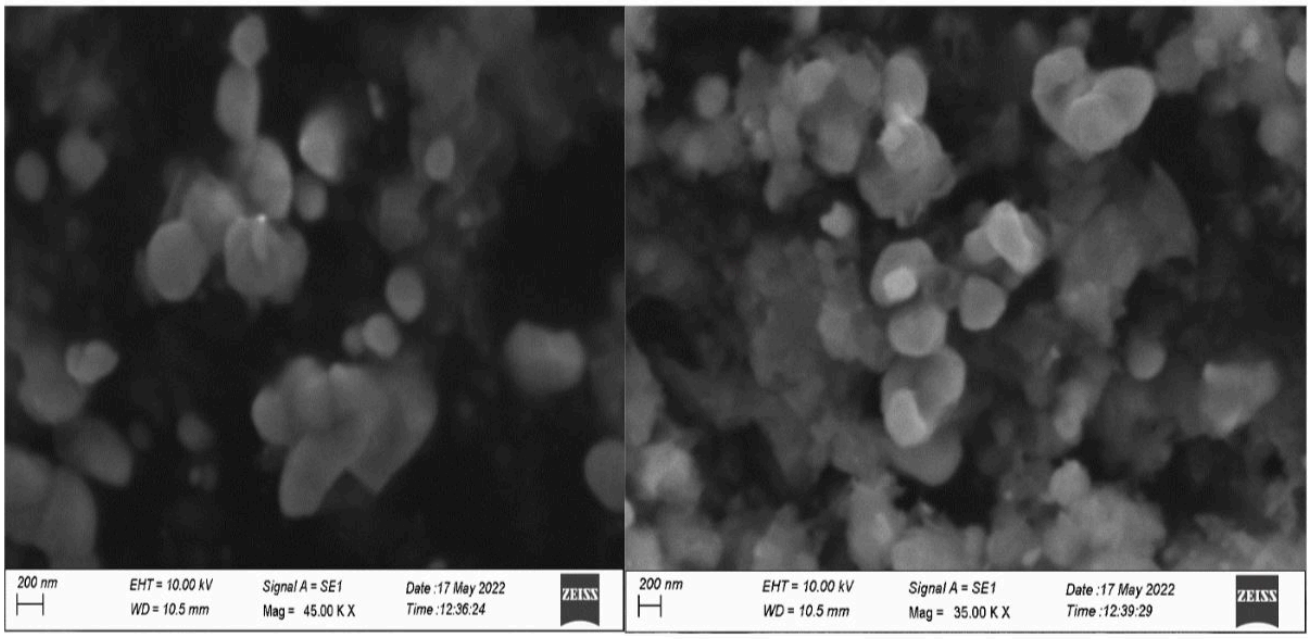

Figure 7

Scanning electron microscopy (SEM) images of silver nanoparticles synthesized using *Phyllanthus emblica*fruit extract at 0.1 M and 0.2 M concentrations, showing spherical morphology and particle distribution.